

# Memory and aging effect in hierarchical spin orderings of the stage-2 $\text{CoCl}_2$ graphite intercalation compound

Masatsugu Suzuki\* and Itsuko S. Suzuki†

*Department of Physics, State University of New York at Binghamton, Binghamton, New York 13902-6000, USA*

Motohiro Matsuura

*Department of Management and Information Science, Fukui University of Technology, Fukui, Fukui 910-8505, Japan*

(Received 27 September 2005; revised manuscript received 4 April 2006; published 11 May 2006)

Stage-2  $\text{CoCl}_2$  graphite intercalation compound undergoes two magnetic phase transitions at  $T_{cl}$  ( $=7.0$  K) and  $T_{cu}$  ( $=8.9$  K). The aging dynamics of this compound is studied near  $T_{cl}$  and  $T_{cu}$ . The intermediate state between  $T_{cl}$  and  $T_{cu}$  is characterized by a spin-glass phase extending over ferromagnetic islands. A genuine thermoremanent magnetization (TRM) measurement indicates that the memory of the specific spin configurations imprinted at temperatures between  $T_{cl}$  and  $T_{cu}$  during the field-cooled (FC) aging protocol can be recalled when the system is reheated at a constant heating rate. The zero-field cooled (ZFC) and TRM magnetization is examined in a series of heating and reheating processes. The magnetization shows both characteristic memory and rejuvenation effects. The time ( $t$ ) dependence of the relaxation rate  $S_{ZFC}(t) = (1/H)dM_{ZFC}(t)/d \ln t$  after the ZFC aging protocol with a wait time  $t_w$  exhibits peaks at two different characteristic times in the intermediate state between  $T_{cl}$  and  $T_{cu}$ . This result indicates the coexistence of two types of ordered domains. The observed aging and memory effects are discussed in terms of the droplet model.

DOI: 10.1103/PhysRevB.73.184414

PACS number(s): 75.40.Gb, 75.50.Lk, 75.30.Kz, 75.30.Gw

## I. INTRODUCTION

Magnetic phase transitions of stage-2  $\text{CoCl}_2$  graphite intercalation compound (GIC) have been extensively studied.<sup>1-11</sup> This compound magnetically behaves like a quasi-two-dimensional (2D)  $XY$ -like ferromagnet with a very weak antiferromagnetic interplanar interaction. The intercalate layers are formed of small islands whose average diameters are on the order of  $450 \text{ \AA}$ . The peripheral chlorine ions at the island boundary provide acceptor sites for charges transferred from the graphite layer to the intercalate layer. This compound undergoes magnetic phase transitions at  $T_{cu}$  ( $=8.9$  K) and  $T_{cl}$  ( $=7.0$  K). The growth of the in-plane spin correlation length  $\xi_a$  is limited by the existence of the islands, making the effective interplanar exchange interaction finite and suppressing the 3D spin ordering to a lower temperature than  $T_{cu}$ . At  $T_{cu}$  a 2D ferromagnetic spin order develops inside each island. Between  $T_{cl}$  and  $T_{cu}$  the 2D ferromagnetic long range order (LRO) is established. The in-plane spin correlation length grows to the order of the island size at  $T_{cl}$ . Below  $T_{cl}$  the system is in a 3D antiferromagnetic phase with the 2D ferromagnetic layers being stacked antiferromagnetically along the  $c$  axis.

However, it seems that such a simple picture for the ordering process below  $T_{cu}$  is not appropriate for the peculiar phenomena observed so far in stage-2  $\text{CoCl}_2$  GIC,<sup>3,5,7-9</sup> which are rather characteristic of the spin-glass (SG) phase. Further it may be also inconsistent with the following experimental results. (i) The absorption  $\chi''$  shows peaks at  $T_{cl}$  and  $T_{cu}$ . The peak at  $T_{cl}$  shifts to the high- $T$  side with increasing ac frequency  $f$ , while the peak at  $T_{cu}$  remains unshifted.<sup>10</sup> (ii) The spin correlation length along the  $c$  axis,  $\xi_c$ , grows rapidly below  $T_{cu}$  but quickly saturates to a constant value of  $22 \text{ \AA}$ , or less than two magnetic layers (the  $c$ -axis repeat distance  $d=12.70 \text{ \AA}$ ).<sup>4</sup>

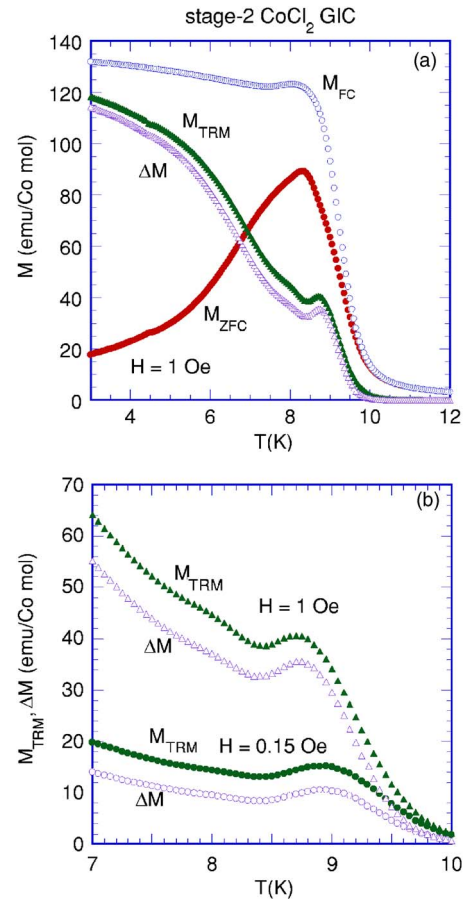


FIG. 1. (Color online) (a)  $T$  dependence of  $M_{ZFC}$ ,  $M_{FC}$ ,  $M_{TRM}$ , and  $\Delta M (=M_{FC} - M_{ZFC})$  for stage-2  $\text{CoCl}_2$  GIC.  $H=1$  Oe. (b)  $T$  dependence of  $M_{TRM}$  at  $H_c=1.0$  and  $0.15$  Oe and  $\Delta M$  at  $H=H_c=1$  and  $0.15$  Oe.  $T_{cu}=8.9$  K.

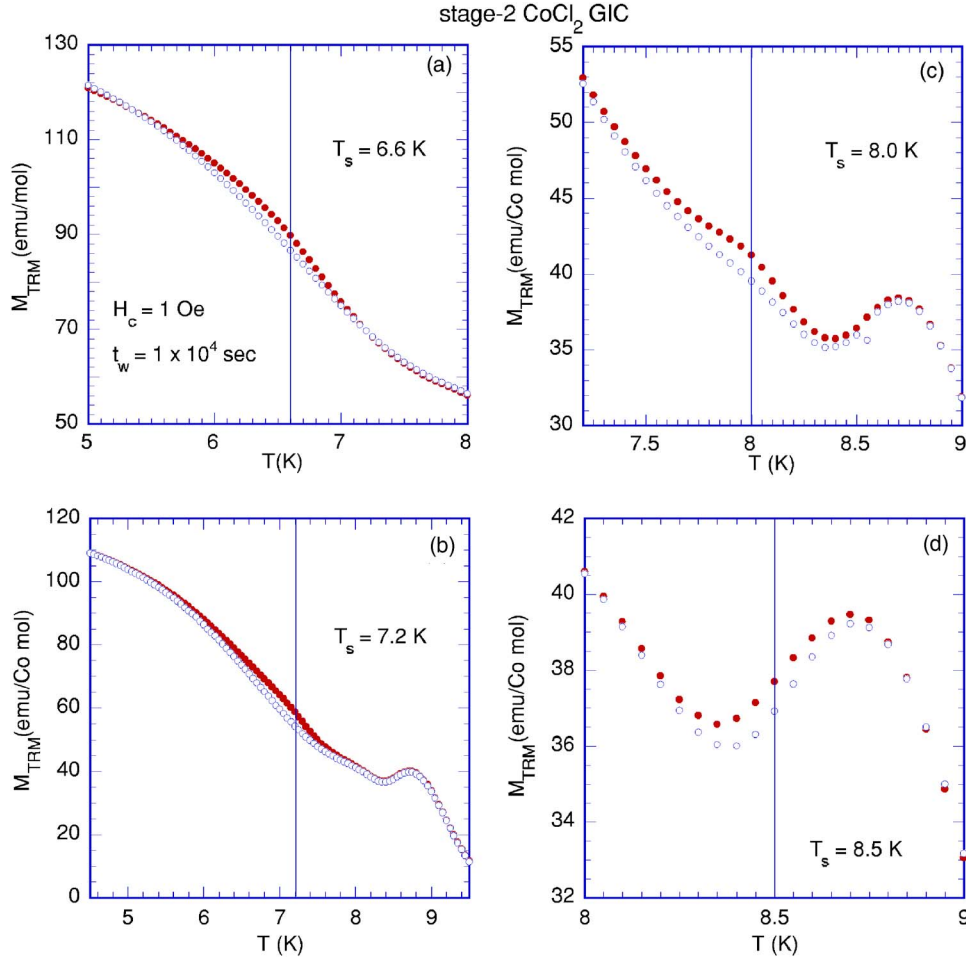


FIG. 2. (Color online)  $T$  dependence of  $M_{\text{TRM}}(T; T_s, t_s)$  (closed circles) and of  $M_{\text{TRM}}^{\text{ref}}(T)$  (open circles).  $M_{\text{TRM}}(T; T_s, t_s)$  is measured with increasing  $T$  at  $H_c=1$  Oe with a stop-wait at  $T_s$  for  $t_s=1.0 \times 10^4$  s.  $M_{\text{TRM}}^{\text{ref}}$  is measured with increasing  $T$  after the FC aging protocol at  $H_c=1$  Oe without such a stop-wait protocol. (a)  $T_s=6.6$  K, (b) 7.2 K, (c) 8.0 K, and (d) 8.5 K.

Under such a circumstance, we performed a series of experiments on the dynamical aspect of the ordering process. Most of them are used to study the aging dynamics (aging, memory and rejuvenation) of SG's. In this paper we study the aging dynamics of stage-2  $\text{CoCl}_2$  GIC near  $T_{cu}$  and  $T_{cl}$ . Our experiments include (i) genuine thermoremanent magnetization (TRM), (ii) relaxation rate of the zero-field cooled (ZFC) magnetization, (iii) ZFC magnetization and TRM magnetization in a series of heating and cooling process which is the same procedure used by Matsuura *et al.*<sup>5</sup> for stage-2  $\text{CoCl}_2$  GIC, and (iv) field-cooled (FC) magnetization in a FC aging protocol (with an intermittent stop for a wait time in the absence of a magnetic field) which is the same protocol used by Sun *et al.*<sup>12</sup> for permalloy ( $\text{Ni}_{81}\text{Fe}_{19}$ ) nanoparticles.

We show that the intermediate state is a SG ordered phase extending over ferromagnetic islands. The magnetization shows both characteristic memory and rejuvenation effects. The time ( $t$ ) dependence of the relaxation rate  $S_{\text{ZFC}}(t) = (1/H)dM_{\text{ZFC}}(t)/d \ln t$  after the ZFC aging protocol with a wait time  $t_w$  exhibits peaks at different characteristic times in the intermediate state between  $T_{cl}$  and  $T_{cu}$ . The observed aging and memory effect will be discussed in terms of the droplet model.<sup>13-15</sup>

## II. EXPERIMENTAL PROCEDURE

A stage-2  $\text{CoCl}_2$  GIC sample was prepared by intercalation of pristine  $\text{CoCl}_2$  into a single crystal of kish graphite in

a  $\text{Cl}_2$  gas atmosphere at 740 Torr for three weeks at 540 °C. The sample used in the present experiment is one used in the previous experiments.<sup>10,11</sup> The dc magnetization and ac magnetic susceptibility were measured using a SQUID magnetometer (Quantum Design, MPMS XL-5) with an ultra low field capability option. Before the measurement, a remnant magnetic field was reduced to zero field (exactly less than 3 mOe) at 298 K. We measured the dc magnetization as a function of temperature after various kinds of cooling protocol. The detail of the cooling protocol for each experiment will be presented in Sec. III. We also measured the time dependence of the ZFC magnetization at various wait times.

## III. RESULT

### A. $T$ dependence of $M_{\text{ZFC}}$ , $M_{\text{FC}}$ , $M_{\text{TRM}}$ , and $\Delta M$ ( $=M_{\text{FC}}-M_{\text{ZFC}}$ )

In the previous paper,<sup>10</sup> we have studied the dynamic aspect of in-plane spin ordering in stage-2  $\text{CoCl}_2$  GIC from both the dispersion  $\chi'$  and absorption  $\chi''$  at  $f=0.1$  Hz acquired using an ac magnetic susceptibility. The absorption  $\chi''$  shows three peaks at  $T=T_{cu}$  ( $=8.9$  K),  $T_{p1}$  ( $=8.4$  K), and  $T_{cl}$  ( $=7.0$  K), while  $\chi'$  has a single peak at  $T_{p1}$ . These results indicate that this compound undergoes two magnetic phase transitions at  $T_{cl}$  and  $T_{cu}$ .

In order to see how these successive magnetic phase transitions are observed in the dc magnetic susceptibility, we

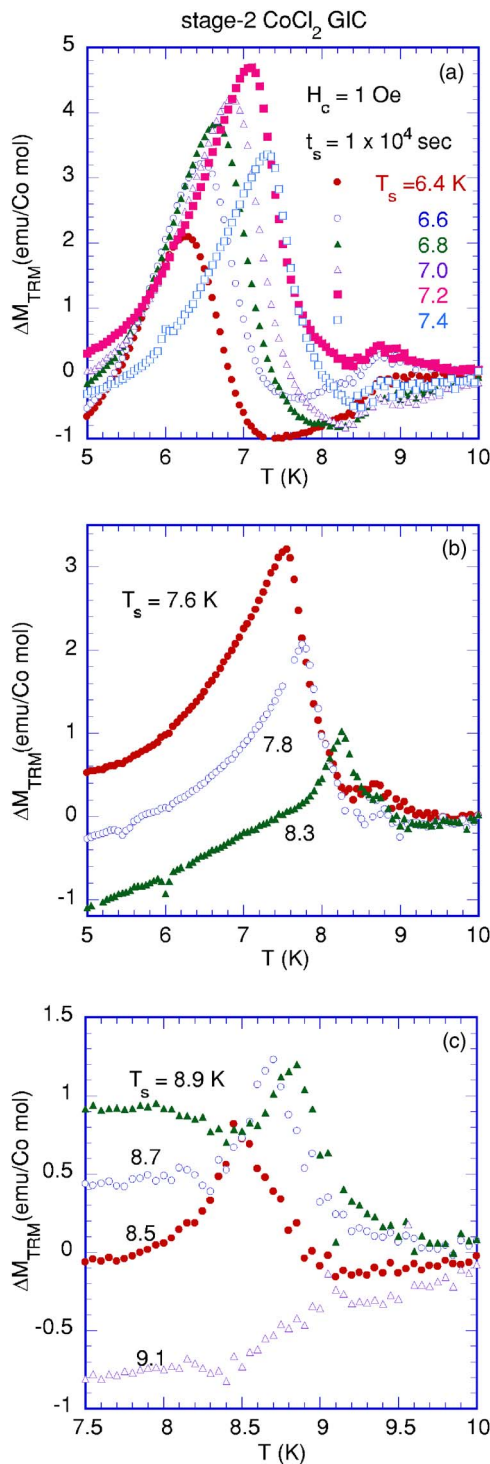


FIG. 3. (Color online)  $T$  dependence of  $\Delta M_{\text{TRM}}(T; T_s, t_s)$  [ $=M_{\text{TRM}}(T; T_s, t_s) - M_{\text{TRM}}^{\text{ref}}(T)$ ].  $t_s = 1.0 \times 10^4$  s.  $6.4 \leq T_s \leq 9.1$  K.  $H_c = 1$  Oe. (a)  $6.6 \leq T \leq 7.4$  K. (b)  $7.6 \leq T \leq 8.3$  K. (c)  $8.5 \leq T \leq 9.1$  K.

measured the temperature ( $T$ ) dependence of the magnetization  $M_{\text{ZFC}}$ ,  $M_{\text{FC}}$ , and  $M_{\text{TRM}}$  in the case of  $H = 1$  and  $0.15$  Oe. (a) *The ZFC magnetization ( $M_{\text{ZFC}}$ ) measurement.* The system was annealed at  $50$  K for  $1.2 \times 10^3$  s in the absence of  $H$ . The system was cooled from  $50$  to  $1.9$  K at  $H = 0$  (ZFC aging protocol). After the system was aged at  $1.9$  K for

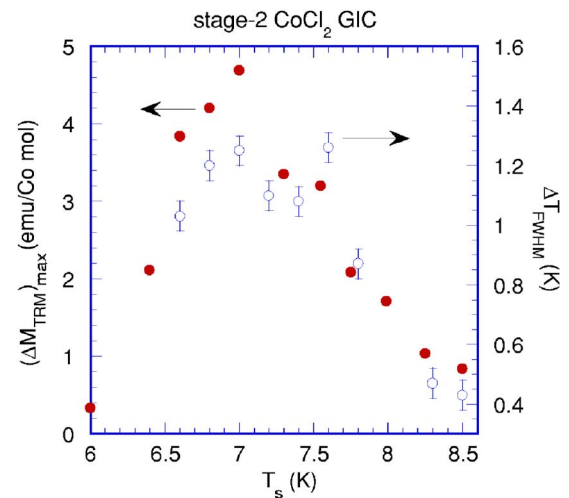


FIG. 4. (Color online)  $T_s$  dependence of the peak height of  $\Delta M_{\text{TRM}}(T; T_s, t_s)$  denoted by  $(\Delta M_{\text{TRM}})_{\text{max}}$ . The curve of  $\Delta M_{\text{TRM}}$  vs  $T$  shows a peak at  $T_s$ .  $T_s$  dependence of the full-width at half-maximum ( $=\Delta T_{\text{FWHM}}$ ) for the peak of the curve of  $\Delta M_{\text{TRM}}$  vs  $T$  located at  $T = T_s$ .

$t_w = 1.0 \times 10^2$  s at  $H = 0$ , the magnetic field is applied at  $H (=1$  and  $0.15$  Oe). Subsequently  $M_{\text{ZFC}}$  was measured with increasing  $T$  from  $1.9$  to  $12$  K at the rate of  $0.025$  K/minute. (b) *The FC magnetization ( $M_{\text{FC}}$ ) measurement.* The system was annealed at  $50$  K for  $1.2 \times 10^3$  s in the presence of  $H (=1$  and  $0.15$  Oe). Then the system was cooled from  $50$  to  $12$  K in the presence of  $H$  (FC aging protocol). The magnetization  $M_{\text{FC}}$  was measured with decreasing  $T$  from  $12$  to  $1.9$  K. (c) *The thermoremanent magnetization ( $M_{\text{TRM}}$ ) measurement.* The system was cooled from  $50$  to  $1.9$  K in the presence of  $H = H_c (=1$  and  $0.15$  Oe) through the FC aging protocol. After the system was aged at  $1.9$  K for  $t_w = 1.0 \times 10^2$  s, the field was cut off ( $H = 0$ ). Then the magnetization  $M_{\text{TRM}}$  was measured with increasing  $T$  from  $1.9$  to  $12$  K. Note that the remnant magnetic field effect on the magnetization curves is corrected.

Figure 1(a) shows the  $T$  dependence of  $M_{\text{ZFC}}$ ,  $M_{\text{FC}}$ ,  $M_{\text{TRM}}$ , and  $\Delta M = M_{\text{FC}} - M_{\text{ZFC}}$  for  $H = 1$  Oe. The magnetization  $M_{\text{ZFC}}$  exhibits a peak at  $8.3$  K close to  $T_{p1}$ , which remains unchanged with decreasing  $H$  from  $1$  to  $0.15$  Oe. The deviation of  $M_{\text{ZFC}}$  from  $M_{\text{FC}}$  starts to occur below  $10.5$  K, due to the irreversibility effect of magnetization. Figure 1(b) shows the  $T$  dependence of  $M_{\text{TRM}}$  for  $H_c = 0.15$  and  $1$  Oe, and  $\Delta M$  for  $H = 0.15$  and  $1$  Oe. The magnetization  $M_{\text{TRM}}$  at  $H_c = 1$  Oe exhibits a local maximum at  $8.70$  K. The local-maximum temperature increases with decreasing  $H_c$  and reaches  $8.85$  K at  $H_c = 0.15$  Oe, which is very close to  $T_{cu}$ . Although  $\Delta M$  at  $H = H_0 (=0.15$  and  $1$  Oe) is smaller than  $M_{\text{TRM}}$  at  $H_c = H_0$ , below  $10$  K, the  $T$  dependence of  $\Delta M$  at  $H = H_0$  is similar to that of  $M_{\text{TRM}}$  at  $H_c = H_0$ . The derivative  $dM_{\text{TRM}}/dT$  exhibits a negative local minimum at  $T = 6.9$  K for  $H_c = 1$  Oe and at  $T = T_{cl} (=7.0$  K) for  $H_c = 0.15$  Oe.

## B. Genuine TRM measurement

We present a memory effect observed in the so-called genuine TRM magnetization measurement of stage-2  $\text{CoCl}_2$



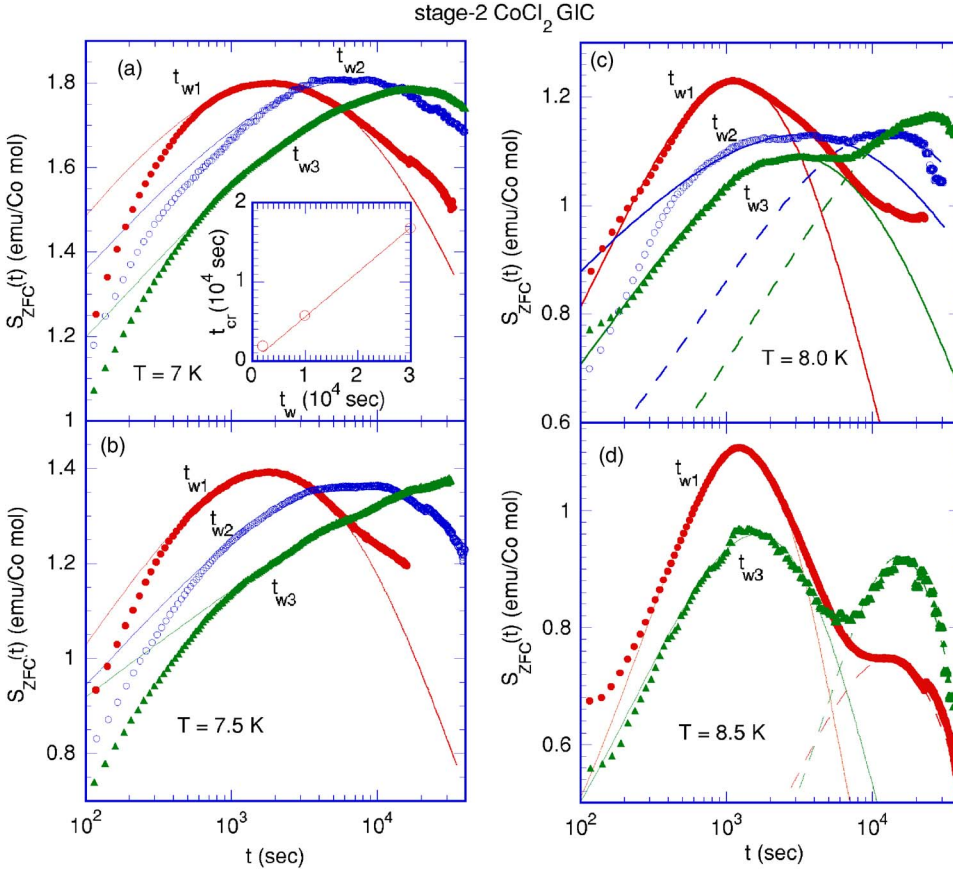


FIG. 5. (Color online)  $t$  dependence of  $S_{ZFC}(t)$  at various  $t_w$  ( $t_{w1}=2.0 \times 10^3$  s,  $t_{w2}=1.0 \times 10^4$  s, and  $t_{w3}=3.0 \times 10^4$  s).  $H=1$  Oe. (a)  $T=7.0$  K, (b) 7.5 K, (c) 8.0 K, and (d) 8.5 K. The lines denote the least-squares fits to a SER given by Eq. (2) for  $S_{ZFC}$  vs  $t$  in the vicinity of the peak time  $t_{cr}$ . The fitting parameters  $\tau$  and  $n$  for each  $T$  are shown in Figs. 6(a) and 6(b). The inset of (a) shows the relation between  $t_{cr}$  and  $t_w$ .

GIC. Similar behavior is observed in SG's.<sup>16–19</sup> Our system was cooled from 50 K to an intermittent stop temperature  $T_s$  ( $6.0 \leq T_s \leq 9.1$  K) in the presence of  $H=H_c$  ( $=1$  Oe) (stop-wait process). The system was aged at  $T_s$  for a wait time  $t_s$  ( $=1.0 \times 10^4$  s) at  $H=H_c$ , and subsequently it was cooled again down to 3.0 K. After the magnetic field was switched off at 3.0 K, the TRM magnetization was measured with increasing  $T$  from 3.0 to 12 K at  $H=0$ . This value of the TRM magnetization is compared with that of the TRM magnetization which was measured with increasing  $T$  after the FC aging protocol without any stop-wait process [ $M_{TRM}^{ref}(T)$  as the reference curve]. Here we define the difference  $\Delta M_{TRM}(T; T_s, t_s)$  as

$$\Delta M_{TRM}(T; T_s, t_s) = M_{TRM}(T; T_s, t_s) - M_{TRM}^{ref}(T). \quad (1)$$

Figure 2 shows the  $T$  dependence of  $M_{TRM}(T; T_s, t_s)$  (stop-wait curve) and  $M_{TRM}^{ref}(T)$  (reference curve) at  $t_s=1.0 \times 10^4$  s for typical stop temperatures ( $T_s=6.6, 7.2, 8.0,$  and  $8.5$  K). The reference curve and the stop-wait curves coalesce at low temperatures and only start to deviate as  $T_s$  is approached from the low  $T$  side. The stop-wait curves lie significantly above the reference curve in the vicinity of  $T_s$ . Figure 3 shows the  $T$  dependence of  $\Delta M_{TRM}(T; T_s, t_s)$  at various  $T_s$ . The difference  $\Delta M_{TRM}(T; T_s, t_s)$  shows either a symmetric broad peak centered at  $T=T_s$  for  $T_s < 7.4$  K or an asymmetric cusp centered at  $T=T_s$  for  $7.6$  K  $< T < T_{cu}$ . The peak of  $\Delta M_{TRM}(T; T_s, t_s)$  is not clearly observed for  $T_s \leq 6.0$  K. The result indicates that the spin configuration im-

printed at  $T_s$  is recovered on reheating. In this sense, the system sustains a memory of an equilibrium state reached after a stop-wait process at  $T_s$ . Such phenomena are commonly observed in various kinds of SG's. Figure 4 shows the  $T_s$  dependence of the peak height of the curve  $\Delta M_{TRM}(T; T_s, t_s)$  vs  $T$  located at  $T_s$  [denoted by  $(\Delta M_{TRM})_{max}$ ]. The peak height exhibits a sharp peak at  $T_s = T_{cl}$ . It decreases with further increasing  $T_s$  and tends to zero around  $T_{cu}$ . As will be discussed in Sec. IV C, the magnetization  $(\Delta M_{TRM})_{max}$  is roughly proportional to  $\xi_a^2$  between  $T_{cl}$  and  $T_{cu}$ . The increase of  $(\Delta M_{TRM})_{max}$  with decreasing  $T$  between  $T_{cl}$  and  $T_{cu}$  suggests that  $\xi_a$  increases with decreasing  $T$  from  $T_{cu}$  to  $T_{cl}$ . In Fig. 4 we also show the  $T_s$  dependence of the full-width at half-maximum [ $=\Delta T_{FWHM}$ ] for the peak of the curve  $\Delta M_{TRM}$  vs  $T$  located at  $T=T_s$ . The full-width at half-maximum  $\Delta T_{FWHM}$  exhibits a peak around  $T_s=T_{cl}$ . It is on the order of 1.2 K at  $T_s=T_{cl}$  and 0.4 K around  $T_s=T_{cu}$ . The  $T_s$  dependence of  $\Delta T_{FWHM}$  will be discussed in terms of the overlap length of the droplet model<sup>13–15</sup> for SG's in Sec. IV D.

### C. Relaxation rate $S_{ZFC}(t)$

We have measured the  $t$  dependence of  $M_{ZFC}(t)$  at the fixed  $T$  for various wait time  $t_w$  ( $t_{w1}=2.0 \times 10^3$  s,  $t_{w2}=1.0 \times 10^4$  s, and  $t_{w3}=3.0 \times 10^4$  s), where  $H=1$  Oe. The measurements were carried out after the ZFC aging protocol: annealing of the system at  $T=50$  K and  $H=0$  for  $1.2 \times 10^3$  s, quenching from 50 K to  $T$  at  $H=0$ , and isothermal aging at  $T$

for  $t_w$ . The origin of  $t$  ( $t=0$ ) is a time just after  $H=1$  Oe is applied at  $T$ . The magnetization  $M_{ZFC}$  increases with increasing  $t$ , depending on  $t_w$  and  $T$ .

Figures 5(a)–5(d) show typical examples of the  $t$  dependence of the relaxation rate  $S_{ZFC}(t) [(1/H)dM_{ZFC}(t)/d \ln t]$  at fixed  $T$  ( $T=7.0, 7.5, 8.0,$  and  $8.5$  K), where  $t_w$  is varied as a parameter. At  $T=7.0$  K [see Fig. 5(a)],  $S_{ZFC}(t)$  exhibits a single peak at a characteristic time  $t_{cr}$ , which shifts to a longer- $t$  side with increasing  $t_w$ . The peak time  $t_{cr}$  is proportional to  $t_w$ :  $t_{cr}/t_w=0.56\pm 0.02$  as shown in the inset of Fig. 5(a). This result reflects the influence of the aging process on the relaxation of the system. Similar aging behavior is observed for  $S_{ZFC}(t)$  at  $T=7.5$  K [see Fig. 5(b)]. Note that no peak is observed for  $S_{ZFC}(t)$  at  $t_w=t_{w3}$  for  $0 < t < t_{w3}$ , indicating that  $t_{cr}$  is at least longer than  $t_{w3}$ . The shape of  $S_{ZFC}(t)$  in the vicinity of  $t=t_{cr}$  is well described by a stretched exponential relaxation (SER) given by

$$S_{ZFC}(t) = S_{\max}^0 e^{(t/\tau)^{1-n}} \exp[-(t/\tau)^{1-n}], \quad (2)$$

where  $\tau$  is the SER relaxation time,  $n$  is the SER exponent,  $S_{\max}^0$  is the peak height, and  $e$  is the base of natural logarithmic. The value of  $\tau$  is equal to that of  $t_{cr}$ . The lines in Figs. 5(a) and 5(b) denote the least-squares fits to the SER given by Eq. (2) for  $S_{ZFC}(t)$  in the vicinity of the peak time  $t_{cr}$ . We note that the deviation of  $S_{ZFC}(t)$  from the SER occurs at  $t \gg t_{cr}$  and  $t \ll t_{cr}$ .

At  $T=8.0$  K [see Fig. 5(c)],  $S_{ZFC}(t)$  for  $t_w=t_{w3}$  exhibits two broad peaks at  $t=t_{cr1}$  ( $=3.2 \times 10^3$  s) and  $t_{cr2}$  ( $=2.5 \times 10^4$  s). The shape of  $S_{ZFC}(t)$  is well described by two SER curves showing peaks around  $t_{cr1}$  and  $t_{cr2}$ . These results suggest the coexistence of correlated domains and isolated single domains (see Sec. IV B). In contrast,  $S_{ZFC}(t)$  at  $t_w=t_{w1} (\ll t_{w3})$  is described by a single SER centered at  $t=t_{cr}=1.1 \times 10^3$  s. Similar behaviors are also observed at  $T=8.5$  K [see Fig. 5(d)] and 9.0 K (the data are not shown in the text).

Figure 6(a) shows the  $T$  dependence of the SER relaxation times  $\tau$  which are determined from the least-squares fit of the data [ $S_{ZFC}(t)$  vs  $t$ ] at various  $t_w$  in the vicinity of the peak times. For  $T \leq T_{cl}$ , there is a single relaxation time  $\tau$  which depends on  $t_w$ . In Fig. 6(a) we show only the  $T$  dependence of  $\tau(t_{w1})$  and  $\tau(t_{w3})$ , which are related to the growth of correlated domains over different  $t_w$  (see Sec. IV B). For  $T_{cl} < T < T_{cu}$ , the relaxation time  $\tau(t_{w3})$  separate into two relaxation times,  $\tau_1(t_{w3})$  for the isolated single domains and  $\tau_2(t_{w3})$  for the correlated domains. The relaxation time  $\tau_1(t_{w3})$  decreases with increasing  $T$ , while  $\tau_2(t_{w3})$  exhibits a peak around  $T=7.5$  K and decreases with further increasing  $T$ . It seems that  $\tau_2(t_{w3})$  diverges as  $T$  is approached  $T_{cl}$  from the high- $T$  side. Note that the relaxation time observed at  $t_w=t_{w2}$  is located on the curve of  $\tau_1(t_{w3})$  vs  $T$ . In contrast, the relaxation time  $\tau(t_{w1})$  continuously decreases with increasing  $T$ , showing a local minimum around  $T=8.0$  K. It coincides with  $\tau_1(t_{w3})$  at  $T=T_{cu}$ .

Figure 6(b) shows the  $T$  dependence of  $n$  determined from the least-squares fit of the data [ $S_{ZFC}(t)$  vs  $t$ ] in the vicinity of  $\tau_2(t_{w3})$ ,  $\tau_1(t_{w3})$ , and  $\tau(t_{w1})$  to Eq. (2), respectively. We find

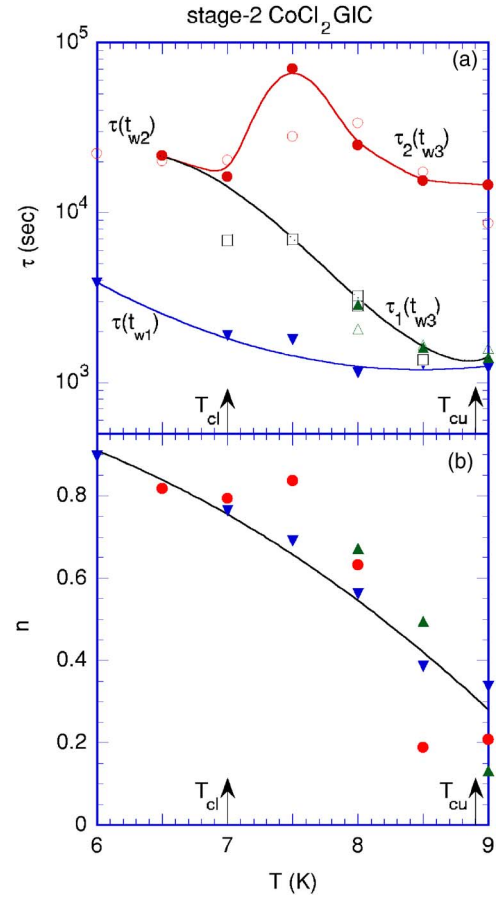


FIG. 6. (Color online)  $T$  dependence of the fitting parameters  $\tau$  and  $n$ .  $H=1$  Oe. (a)  $\tau$  vs  $T$  and (b)  $n$  vs  $T$  at various  $t_w$  [ $t_w=t_{w1}$  ( $\blacktriangledown$ ),  $t_{w2}$  ( $\square$ ),  $t_{w3}$  ( $\bullet$ ,  $\blacktriangle$ ,  $\circ$ ,  $\triangle$ )]. For  $t_w=t_{w3}$ , two SER peaks are observed at  $t < 3.0 \times 10^3$  s ( $\blacktriangle$ ,  $\triangle$ ) and  $t > 1.0 \times 10^4$  s ( $\bullet$ ,  $\circ$ ) above 8.0 K.  $\tau$  is equal to the peak time  $t_{cr}$  of the curve  $S_{ZFC}(t)$  vs  $t$  at the fixed  $T$ . In order to check the reproducibility of the data at  $t_w=t_{w3}$ , the measurements were carried out twice independently:  $n$  and  $\tau$  ( $\circ$ ,  $\triangle$ ) for the first measurement and  $\tau$  ( $\bullet$ ,  $\blacktriangle$ ) for the second measurement. The data of Figs. 5(a) and 5(b) correspond to those of the second measurement. The arrows indicate the location of  $T_{cl}$  and  $T_{cu}$ .

that  $n$  is well described by a single function of  $T$ , in spite of the different SER forms at  $\tau_2(t_{w3})$ ,  $\tau_1(t_{w3})$ , and  $\tau(t_{w1})$ . The exponent  $n$  is characterized by the large value of  $n$  below  $T_{cl}$  and the decrease of  $n$  with increasing  $T$ :  $n=0.78\pm 0.01$  at  $T=T_{cl}$  and  $n\approx 0.28$  at  $T=T_{cu}$ . These features are in agreement with those reported in typical spin-glass systems such as  $\text{Eu}_{0.4}\text{Sr}_{0.6}\text{S}$  ( $n=0.83$  at  $T_{SG}=1.3$  K, the spin freezing temperature  $T_{SG}=1.5$  K) (Refs. 20 and 21) and  $\text{Cu}_{0.5}\text{Co}_{0.5}\text{Cl}_2\text{-FeCl}_3$  graphite bi-intercalation compound ( $n=0.85$  at  $T=3.3$  K,  $T_{SG}=3.92$  K).<sup>22</sup> In both systems,  $n$  decreases with increasing  $T$  and is nearly equal to 0.70 at  $T=T_{SG}$ .

#### D. Memory effect for $M_{TRM}$ and $M_{ZFC}$

Here we present our result on memory phenomena of  $M_{TRM}$  and  $M_{ZFC}$  for stage-2 CoCl<sub>2</sub> GIC, which is observed in a series of heating and cooling processes. Such a character-

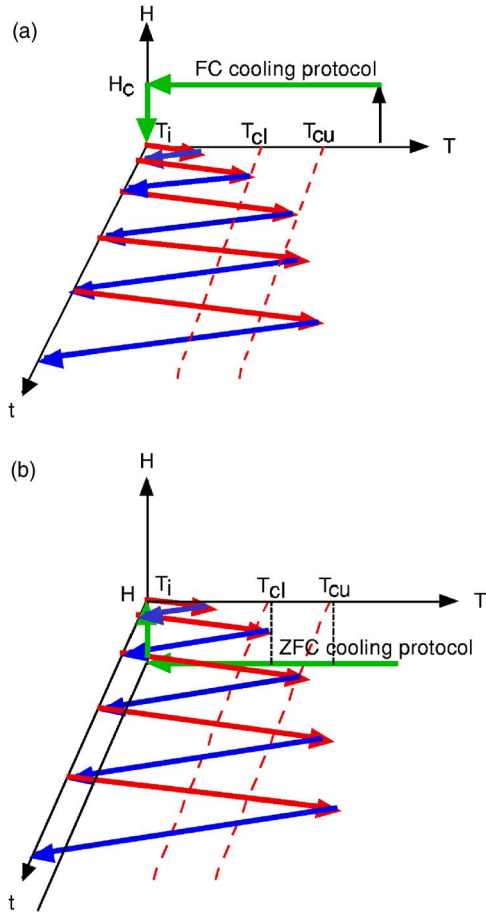


FIG. 7. (Color online) (a) TRM case. Repeated processes of heating from  $T_i=3.0$  K to  $T_r$  (U-turn temperature), cooling from  $T_r$  to  $T_i$ , and reheating from  $T_i$  K to  $T_{r+1}$  ( $>T_r$ ) in the absence of  $H$ , after the FC aging protocol (quenching from 50 K to  $T_i$  at  $H=H_c=1$  Oe and annealing at  $T_i$  for  $1.0 \times 10^2$  s). (b) ZFC case. Repeated processes of heating from  $T_i=3.0$  K to  $T_r$  (U-turn temperature), cooling from  $T_r$  to  $T_i$ , and reheating from  $T_i$  to  $T_{r+1}$  ( $>T_r$ ) in the presence of  $H$  ( $=1$  Oe), after the ZFC aging protocol (quenching from 50 K to  $T_i$  at  $H=0$  and aging at  $T_i$  for  $1.0 \times 10^2$  s).

istic phenomenon has been predicted theoretically in SG based on a successive bifurcation model of the energy level scheme below the spin freezing temperature.<sup>5</sup>

(i) *TRM case*: Before the TRM magnetization measurement, a FC aging protocol was carried out, consisting of (a) annealing of the system at 50 K for  $1.2 \times 10^3$  s in the presence of  $H$  ( $=1$  or  $0.15$  Oe), (b) quenching of the system from 50 K to  $T=T_i=3.0$  K, and (c) aging the system at  $T=T_i$  at  $H$  for a wait time  $t_w=1.0 \times 10^2$  s. Just after the magnetic field was turned off, the TRM magnetization was measured with increasing  $T$  from  $T_i$  ( $=3.0$  K) to  $T_1$  ( $=4.5$  K) (the first U-turn temperature) and subsequently with decreasing  $T$  from  $T_1$  to  $T_i$  (the cooling process). In turn, it was measured with increasing  $T$  from  $T_i$  to  $T_2$  ( $=5.0$  K) (the heating process) and subsequently with decreasing  $T$  from  $T_2$  to  $T_i$  (the cooling process). This process was repeated for the U-turn temperatures  $T_r$  ( $r=3-11$ ), where  $T_r > T_i$ . The schematic diagram of these processes for the TRM measurement is also shown in Fig. 7(a).

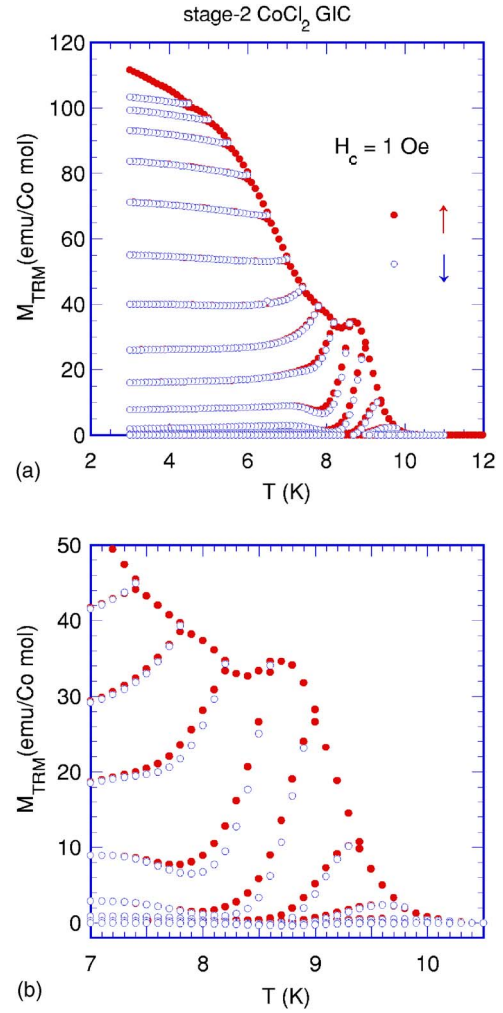


FIG. 8. (Color online) (a) and (b)  $T$  dependence of  $M_{\text{TRM}}$  measured at  $H=0$  in a series of heating (closed circles) and cooling (open circles) processes [see Fig. 7(a) and text for detail] after the FC aging protocol of the system from 50 to  $T_i=3.0$  K in the presence of  $H_c$  ( $=1$  Oe). Note that the data of  $M_{\text{TRM}}$  shown here are corrected one by the subtraction of the data of  $M_{\text{TRM}}$  vs  $T$  obtained with decreasing  $T$  from  $T_f$  ( $=12$  K) to  $2.0$  K, which may be affected by the remanent magnetic field ( $\approx 3$  m Oe).

Figures 8(a) and 8(b) show typical examples of the  $T$  dependence of  $M_{\text{TRM}}$  obtained using the above procedure, where  $H_c=1$  Oe. The value of  $M_{\text{TRM}}$  lies between those of  $M_{\text{TRM}}^{\text{ref}}$  and  $M=0$  line at any  $T$  below  $T_{cu}$ . Here the magnetization  $M_{\text{TRM}}^{\text{ref}}$  is measured with increasing  $T$  from  $T_i$  to 12 K at  $H=0$  after the FC aging protocol at  $H=H_c=1$  Oe. Figure 9 shows typical examples of the path of  $M_{\text{TRM}}$  vs  $T$  obtained in both the cooling process ( $T=T_r \rightarrow T_i$ ) and the heating process ( $T=T_i \rightarrow T_r$ ), where  $T_r=7.0, 7.4, 7.8, 8.2, 8.6,$  and  $8.9$  K. Figure 10(a) shows the  $T_r$  dependence of  $M_r$  and  $M_i$ , where  $M_r$  and  $M_i$  are the values of  $M_{\text{TRM}}$  at  $T=T_r$  and  $T_i$  in the cooling process ( $T=T_r \rightarrow T_i$ ), respectively. Figure 10(b) shows the  $T_r$  dependence of the derivative  $dM_i/dT_r$ . It exhibits a negative local minimum at  $T_r=T_{cl}=7.0$  K. Figure 10(c) shows the difference  $\Delta M_{ir}^{\text{TRM}}$  ( $=M_i-M_r$ ) which is derived from Fig. 10(a). For  $T_r < 7.0$  K, the path of  $M_{\text{TRM}}(T \downarrow)$  in the cooling process ( $T=T_r \rightarrow T_i$ ) is almost the same as that



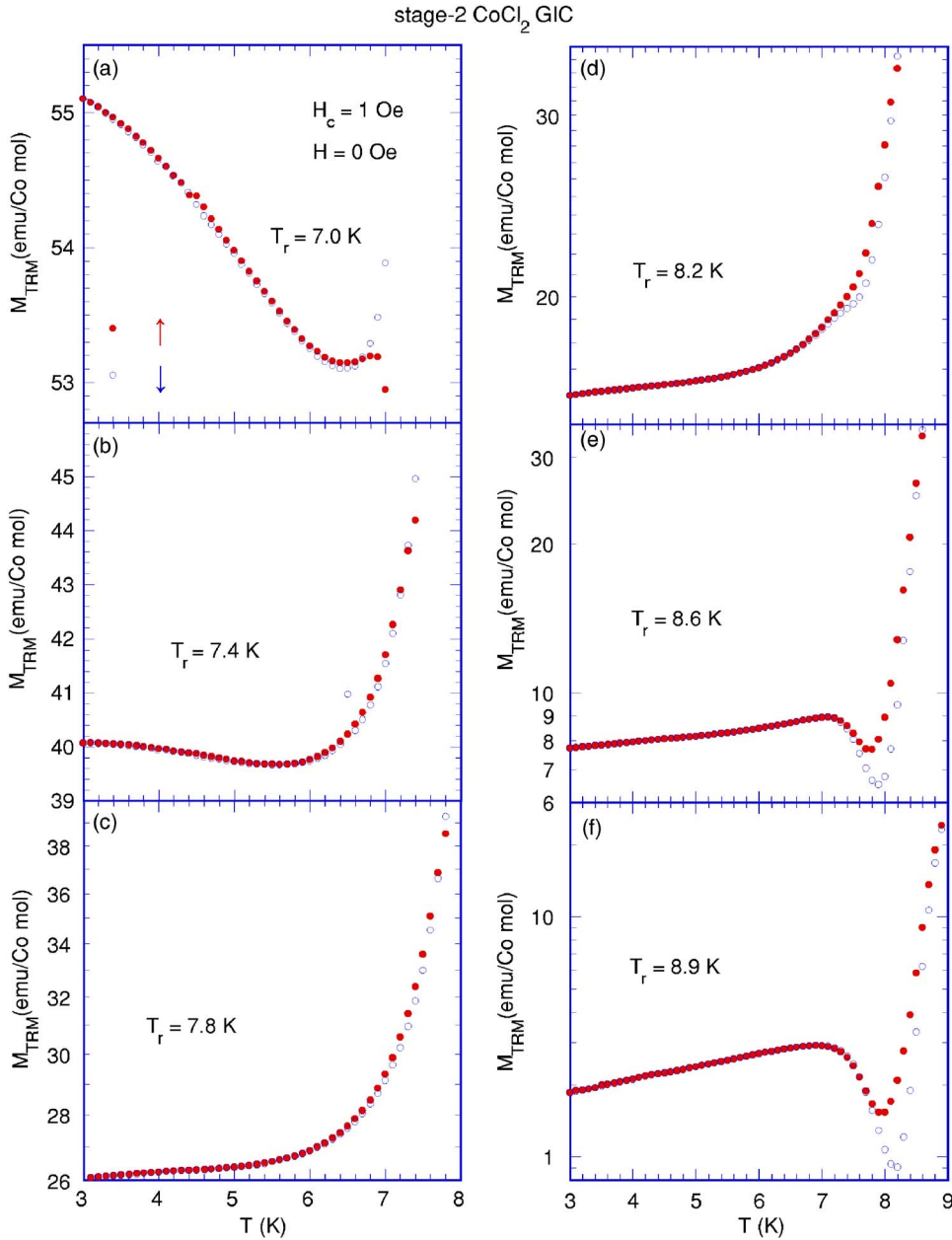


FIG. 9. (Color online)  $T$  dependence of  $M_{\text{TRM}}$  at  $H=0$  which is measured with decreasing  $T$  from  $T_r$  to  $T_i=3.0$  K [ $M_{\text{TRM}}(T\downarrow)$ , open circles] and subsequently measured with increasing  $T$  from  $T_i$  to  $T_r$  [ $M_{\text{TRM}}(T\uparrow)$ , closed circles]. (a)  $T_r=7.0$  K, (b) 7.4 K, (c) 7.8 K, (d) 8.2 K, (e) 8.6 K, and (f) 8.9 K.

of  $M_{\text{TRM}}(T\uparrow)$  in the heating process ( $T=T_i \rightarrow T_r$ ) indicating that  $M_{\text{TRM}}$  vs  $T$  curve is reversible on cooling and heating. For  $T_r \geq 7.8$  K, however, the  $M_{\text{TRM}}$  vs  $T$  curve is irreversible in the cooling and heating processes. For  $T_r=8.6$  and 8.9 K, the curve of  $M_{\text{TRM}}$  vs  $T$  shows a broad peak around  $T_{cl}$  and a local minimum between  $T_{cl}$  and  $T_{cu}$  in both the cooling and heating processes between  $T_{cl}$  and  $T_{cu}$ . Figure 11(a) shows the difference  $\Delta M_{\text{TRM}} [=M_{\text{TRM}}(T\uparrow) - M_{\text{TRM}}(T\downarrow)]$  as a function of  $T$  for various  $T_r$ . The difference  $\Delta M_{\text{TRM}}$  exhibits a positive peak at a characteristic temperature  $T_p^{\text{TRM}}$  below  $T_r$ . The peak temperature  $T_p^{\text{TRM}}$  linearly increases with increasing  $T_r$  through the relation  $T_p^{\text{TRM}} - T_r = -0.3$  K for  $7.8 \leq T_r \leq 8.9$  K.

The intermediate state between  $T_{cl}$  and  $T_{cu}$  has characteristics of both ordered and disordered states, because of the following reasons. As shown in Fig. 10(c),  $\Delta M_{ir}^{\text{TRM}}$  is positive (or  $M_i > M_r$ ) for  $T_r < T_{cl}$ . It becomes zero when  $T_r$  is

nearly equal to  $T_{cl}$ , and takes a negative local minimum at  $T_r = T_{cu}$ . The disordered nature of the intermediate state is characterized by the negative value of  $\Delta M_{ir}^{\text{TRM}}$  (or  $M_i < M_r$ ). Thus the intermediate state is a sort of disordered state. This feature is in contrast to that of  $\Delta M_{ir}^{\text{TRM}} > 0$  for a FM state of normal ferromagnets. However, the intermediate state also exhibits a memory effect which is one of the main features of the ordered state. The value of  $M_{\text{TRM}}$  at  $T_r$  almost remains unchanged after the cooling process from  $T_r$  to  $T_i$  and the heating process from  $T_i$  to  $T_r$ . In this sense, the intermediate state is a sort of ordered state: SG ordered phase extending over ferromagnetic islands.

(ii) *ZFC case*: Before the ZFC magnetization measurement, a ZFC aging protocol was carried out. It consists of the following process: (a) annealing of the system at 50 K for  $1.2 \times 10^3$  s in the absence of  $H$ , (b) quenching of the system from 50 K to  $T_i=3.0$  K, and (c) aging at  $T_i$  and  $H=0$  for a

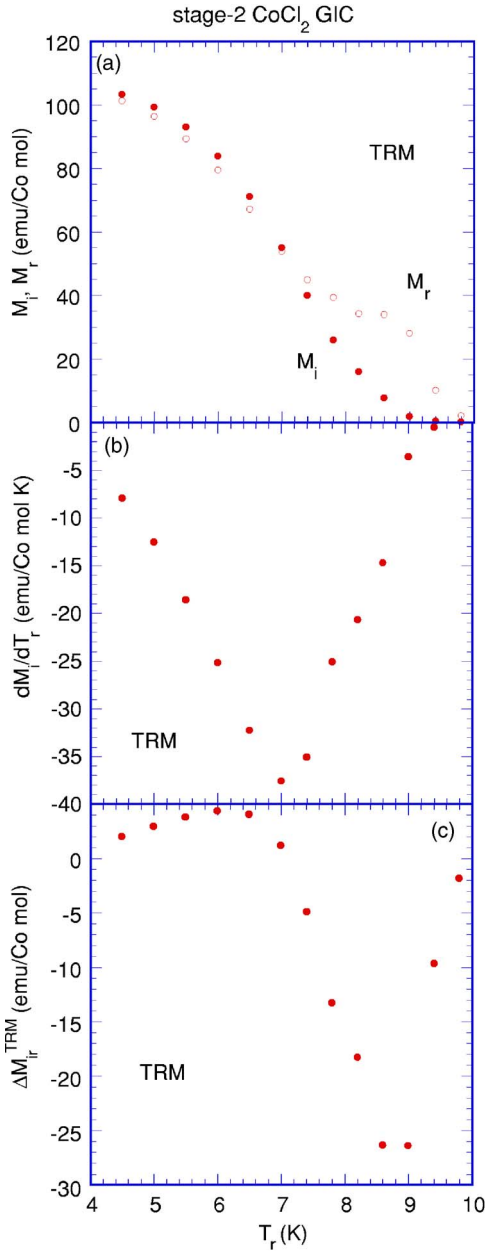


FIG. 10. (Color online) (a)  $T_r$  dependence of  $M_r$  and  $M_i$ .  $M_r$  and  $M_i$  are the value of  $M_{TRM}$  at  $T=T_r$  and  $T_i$  ( $=3.0$  K), respectively, which are obtained in the measurement of  $M_{TRM}$  with decreasing  $T$  from  $T_r$  to  $T_i$  [see Fig. 8(a)]. (b)  $T_r$  dependence of  $dM_i/dT_r$ . (c)  $T_r$  dependence of  $\Delta M_{ir}^{TRM}$  ( $=M_i-M_r$ ).

wait time  $t_w=1.0 \times 10^2$  s. Just after the magnetic field ( $H=1$  Oe) is applied to the system, the ZFC magnetization  $M_{ZFC}$  was measured using the same procedure of heating and cooling:  $T_i \rightarrow T_1 \rightarrow T_i \rightarrow T_2 \rightarrow T_i \rightarrow T_3 \rightarrow T_i \rightarrow \dots$  and so on, where  $T_r$  ( $r=1, 2, \dots$ ) is the U-turn temperature and  $T_r > T_i$ . The schematic diagram of these processes is shown in Fig. 7(b). Figures 12(a) and 12(b) show the  $T$  dependence of  $M_{ZFC}$  using the above method. Note that the value of  $M_{ZFC}$  lies between those of  $M_{ZFC}^{ref}$  and  $M_{FC}^{ref}$  at any  $T$  below  $T_{cur}$ . Here  $M_{ZFC}^{ref}$  is measured with increasing  $T$  from  $T_i$  to 12 K at  $H=1$  Oe after the ZFC aging protocol. The magnetization  $M_{FC}^{ref}$  is measured with decreasing  $T$  from 12 K to  $T_i$  in the

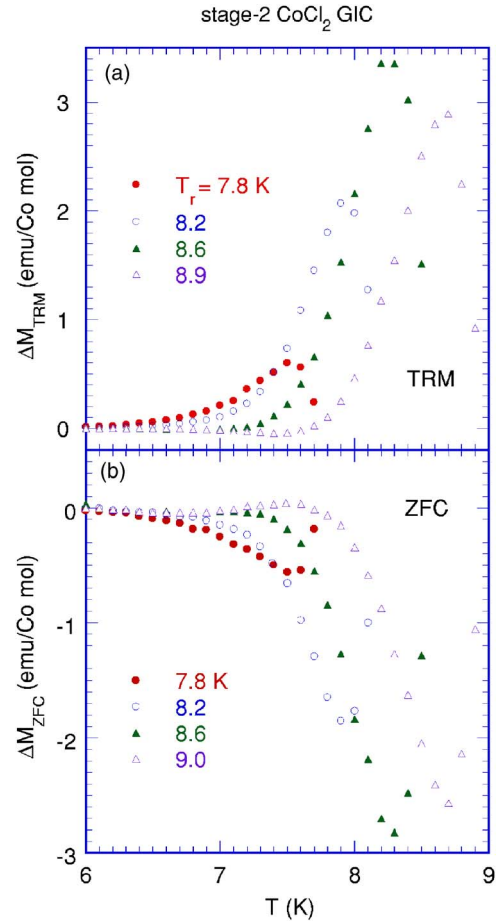


FIG. 11. (Color online) (a)  $T$  dependence of  $\Delta M_{TRM}$  [ $=M_{TRM}(T\uparrow)-M_{TRM}(T\downarrow)$ ] for  $6.0 \text{ K} \leq T \leq T_r$ .  $T_r=7.8, 8.2, 8.6,$  and  $8.9$  K. (b)  $T$  dependence of  $\Delta M_{ZFC}$  [ $=M_{ZFC}(T\uparrow)-M_{ZFC}(T\downarrow)$ ] for  $6.0 \text{ K} \leq T \leq T_r$ .  $T_r=7.8, 8.2, 8.6,$  and  $9.0$  K.

presence of  $H$  ( $=1$  Oe). Figure 13 shows typical examples of the path of  $M_{ZFC}$  vs  $T$  obtained in both the cooling process ( $T=T_r \rightarrow T_i$ ) and the heating process ( $T=T_i \rightarrow T_r$ ), where  $T_r=7.8, 8.2, 8.6,$  and  $9.0$  K. For  $T_r \leq 7.4$  K, the path of  $M_{ZFC}(T\downarrow)$  in the cooling process ( $T=T_r \rightarrow T_i$ ) is the same as that of  $M_{ZFC}(T\uparrow)$  in the heating process ( $T=T_i \rightarrow T_r$ ), indicating that  $M_{ZFC}$  vs  $T$  curve is reversible on cooling and heating. For  $T_r \geq 7.8$  K, however,  $M_{ZFC}(T)$  is irreversible in the cooling and heating processes. For  $T_r \geq 9.2$  K, both the path of  $M_{ZFC}(T\downarrow)$  in the cooling process ( $T=T_r \rightarrow T_i$ ) and the path of  $M_{ZFC}(T\uparrow)$  in the heating process ( $T=T_i \rightarrow T_r$ ) coincide with that of  $M_{FC}^{ref}$  which is obtained by cooling from the PM phase to  $T=T_i$  in the presence of  $H$  ( $=1$  Oe).

Figure 14(a) shows the  $T_r$  dependence of  $M_r$  and  $M_i$ , where  $M_r$  and  $M_i$  are the values of  $M_{ZFC}$  at  $T=T_r$  and  $T_i$  in the cooling process ( $T=T_r \rightarrow T_i$ ), respectively. Figure 14(b) shows the  $T_r$  dependence of the derivative  $dM_i/dT_r$ . It exhibits a local maximum at  $T_r=T_{cl}=7.0$  K. Figure 14(c) shows the difference  $\Delta M_{ir}^{ZFC}$  ( $=M_i-M_r$ ) which is derived from Fig. 14(a). For  $T_r < T_{cl}$ ,  $\Delta M_{ir}^{ZFC}$  is positive but is nearly equal to zero,  $M_i \approx M_r$ . At  $T_r=T_{cl}$ ,  $\Delta M_{ir}^{ZFC}$  starts to increase with increasing  $T_r$ . At  $T_r \approx 8.2$  K where  $M_r$  exhibits a peak,  $\Delta M_{ir}^{ZFC}$  drastically increases with further increasing  $T_r$ . For



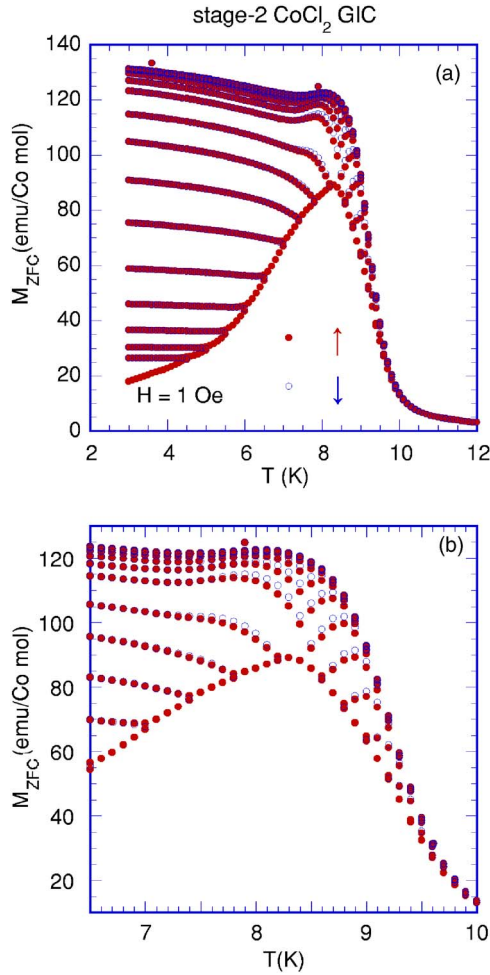


FIG. 12. (Color online) (a) and (b)  $T$  dependence of  $M_{ZFC}$  measured at  $H=1$  Oe in a series of heating (closed circles) and cooling (open circles) processes [see Fig. 7(b) and the text for detail], after the ZFC cooling of the system from 50 to 3.0 K in the absence of  $H$ .

$T_r > T_{cu}$ ,  $M_i$  reaches the equilibrium value. Note that  $M_i$  is 56% value at  $T_r = T_{cl}$  and 98% at  $T_r = T_{cu}$  of the equilibrium value. This result also supports that the intermediate state has the nature of the ordered state.

Figure 11(b) shows the difference  $\Delta M_{ZFC} [=M_{ZFC}(T\uparrow) - M_{ZFC}(T\downarrow)]$  as a function of  $T$  for various  $T_r$ . The difference  $\Delta M_{ZFC}$  exhibits a negative local minima at a characteristic temperature  $T_p^{ZFC}$  below  $T_r$ . The  $T$  dependence of  $\Delta M_{ZFC}$  is almost the same as that of  $-\Delta M_{TRM}$ . Note that  $T_p^{ZFC}$  for the ZFC process is exactly the same as  $T_p^{TRM}$  for the TRM process at the same  $T_r$ . In other words, the magnetization gained in the TRM process corresponds to the magnetization lost in the ZFC process. This result supports the fundamental relation

$$M_{ZFC}(t_w, t) = M_{FC}(0, t + t_w) - M_{TRM}(t_w, t), \quad (3)$$

between the time relaxation of TRM, FC, and ZFC magnetization at low  $H$  in SG's.<sup>23</sup> Similar behavior is observed in the genuine TRM and ZFC measurements of spin-glass Ag(11 at. % Mn).<sup>16</sup>

### E. Memory effect for $M_{FC}$

We present a peculiar memory effect observed in our system using a unique FC aging protocol. Similar behavior is observed in SG's and superparamagnets.<sup>12,24</sup> The result is shown in Fig. 15. First our system was cooled through the FC aging protocol from 50 K to intermittent stop temperatures  $T_s$  ( $=8.5, 6.5, 4.5$  K) in the presence of  $H_c=1$  Oe. When the system was cooled down to each  $T_s$ , the field was cut off ( $H=0$ ) and aged at  $T_s$  for  $t_w$  ( $=3.0 \times 10^4$  s). In this case, the magnetization  $M_{FC}^{IS}(T\downarrow)$  decreases with time due to the relaxation. After the wait time  $t_w$  at  $T_s$ , the field ( $H_c=1$  Oe) was applied again and the FC aging process was resumed. Such a FC aging process leads to a steplike behavior of  $M_{FC}^{IS}(T\downarrow)$  curve. The value of  $M_{FC}^{IS}(T\downarrow)$  after resuming below the lowest stop temperature behaves almost in parallel to that of the FC magnetization without the intermittent stops (as reference curve). After reaching 1.9 K, the magnetization  $M_{FC}^{IS}(T\uparrow)$  was measured in the presence of  $H$  ( $=1$  Oe) as the temperature is increased at the constant rate (0.05 K/min). The magnetization  $M_{FC}^{IS}(T\uparrow)$  thus measured exhibits a broad peak at a characteristic temperature  $T_a=5.3$  K and a peak at  $T_a=7.9$  K. The spin configuration imprinted at the intermittent stop at  $T_s$  for a wait time  $t_w$  at  $H=0$  during the FC aging process strongly affects the  $T$  dependence of  $M_{FC}^{IS}(T\uparrow)$  when the temperature is increased, exhibiting a peculiar memory effect. Figure 15(c) shows the  $T$  dependence of the difference  $\Delta M_{FC}^{IS}$  between  $M_{FC}^{IS}(T\uparrow)$  and  $M_{FC}^{IS}(T\downarrow)$ . Such an oscillatory behavior in  $\Delta M_{FC}^{IS}$  has been reported in superparamagnets, superspin glasses, and spin glasses. Sasaki *et al.*<sup>24</sup> have shown that the aging and memory effects originate solely from a broad distribution of relaxation times. This model may be true for the SG phase extending over ferromagnetic islands. When the field is cut off at  $T=T_s$  for  $t_s$  ( $=3.0 \times 10^4$  s), the magnetic moments of the system formed of small islands whose relaxation times are longer than  $t_s$  are frozen in when the cooling is restarted. These frozen states are reactivated when the system is reheated at  $T_s$ .

## IV. DISCUSSION

### A. Ordered and disordered nature of intermediate state

From our result on the memory effect for  $M_{TRM}$  presented in Sec. III D, we find that the intermediate state between  $T_{cl}$  and  $T_{cu}$  has characteristics of both ordered and disordered states. The disordered nature of the intermediate state is characterized by the negative value of  $\Delta M_{ir}^{TRM}$  (or  $M_i < M_r$ ). This feature is in contrast to that of  $\Delta M_{ir}^{TRM} > 0$  for a ferromagnetic state of normal ferromagnets. However, the intermediate state also exhibits a memory effect as an ordered state. The value of  $M_{TRM}$  at  $T_r$  almost remains unchanged after the cooling process from  $T_r$  to  $T_i$  and the heating process from  $T_i$  to  $T_r$ . In this sense, the intermediate state is a sort of ordered state. Such a characteristic phenomenon is explained in terms of intermediate state with intrainland order and partial interisland order. But if the intermediate state is a completely interisland-disorder state, then thermal equilibrium  $M_{TRM}$  in the state should be always zero. The memory effects observed here indicate that the intermediate state is a SG phase

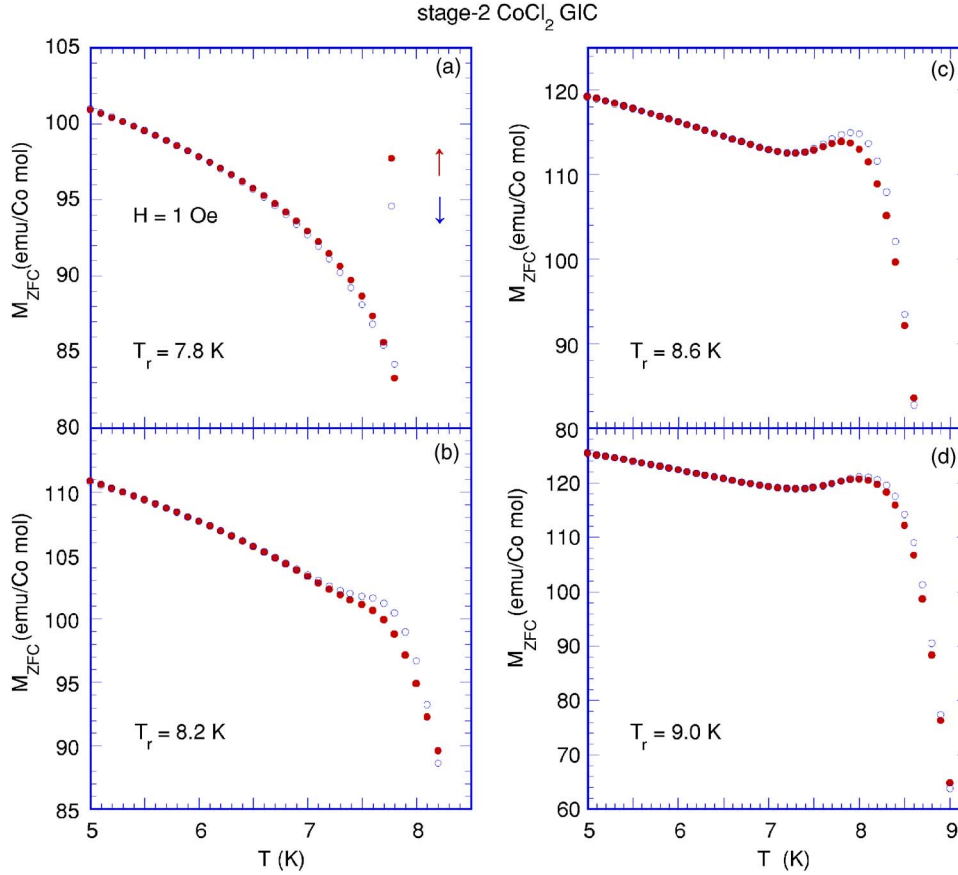


FIG. 13. (Color online)  $T$ -dependence of  $M_{ZFC}$  at  $H=1$  Oe measured with decreasing  $T$  from  $T_r$  to  $T_i$  ( $=3.0$  K) [ $M_{ZFC}(T\downarrow)$ , open circles] and subsequently measured with increasing  $T$  from  $T_i$  to  $T_r$  [ $M_{ZFC}(T\uparrow)$ , closed circles]. (a)  $T_r=7.8$ , (b) 8.2, (c) 8.6, and (d) 8.9 K.

extending over islands, where each island is ferromagnetically ordered. The observed characteristic two-step ordering could be understood thermodynamically as a hierarchy one that the SG phase extending over islands occurs at  $T_{cu}$  and the 3D order occurs at  $T_{cl}$  as an equilibrium state, due to the enhanced interplanar interaction.

### B. The domain size from the relaxation rate $S_{ZFC}(t)$

The aging behavior of  $S_{ZFC}(t)$  after the ZFC aging protocol can be understood in terms of the droplet model.<sup>13-15</sup> The ZFC aging protocol process is completed at  $t_a=0$ , where  $t_a$  is defined as an age (the total time after the ZFC aging protocol process). Then the system is aged at  $T$  under  $H=0$  until  $t_a=t_w$ , where  $t_w$  is a wait time. Correspondingly, the size of domain defined by  $R_T(t_a)$  grows with the age  $t_a$  and reaches  $R_T(t_w)$  just before the field is turned on at  $t=0$  or  $t_a=t_w$ . The aging behavior in  $M_{ZFC}(t)$  is observed as a function of the observation time  $t$ . After  $t=0$ , a probing length  $L_T(t)$  corresponding to the maximum size of excitation grows with  $t$ , in a similar way as  $R_T(t_a)$ . When  $L_T(t) \ll R_T(t_w)$ , quasiequilibrium dynamics is probed, but when  $L_T(t) \gg R_T(t_w)$ , nonequilibrium dynamics is probed. It is predicted that the relaxation rate  $S_{ZFC}(t)$  exhibits a peak when  $t=t_w$ .<sup>25</sup>

In Sec. III C we show that  $S_{ZFC}(t)$  exhibits two peaks at  $t=\tau_1(t_{w3})$  and at  $t=\tau_2(t_{w3})$  in the intermediate state, where  $t_{w3}=3.0 \times 10^4$  s. The  $T$  dependence of  $\tau_1(t_{w3})$  and  $\tau_2(t_{w3})$  is shown in Fig. 6(a). The time  $\tau_2(t_{w3})$  is much longer than  $\tau_1(t_{w3})$  just below  $T_{cu}$ . The ratio  $\zeta [= \tau_2(t_{w3})/\tau_1(t_{w3})]$  is nearly

independent of  $T$  between 8.0 and 9.0 K:  $\zeta=8.7$  at  $T=8.0$  K and 10.4 at  $T=9$  K, respectively. These results suggest that two kinds of characteristic domains with sizes  $L_T[t=\tau_1(t_{w3})]$  and  $L_T[t=\tau_2(t_{w3})]$  coexist in the system. The domain size  $L_T[t=\tau_1(t_{w3})]$  may correspond to the size of isolated small island (domain) just below  $T_{cu}$ . The domain size  $L_T[t=\tau_1(t_{w3})]$  increases as  $T$  approaches  $T_{cl}$  from the high- $T$  side. In contrast, the size  $L_T[t=\tau_2(t_{w3})]$  is much larger than the size  $L_T[t=\tau_1(t_{w3})]$  just below  $T_{cu}$ . These domains may be formed of several small islands through the interisland interactions. The domain size  $L_T[t=\tau_2(t_{w3})]$  increases with decreasing  $T$  below  $T_{cu}$  and takes a maximum at  $T=7.5$  K. The decrease of  $L_T[t=\tau_2(t_{w3})]$  between  $T_{cl}$  and 7.5 K may be related to the frustrated nature of the antiferromagnetic interplanar interactions between domains between adjacent intercalate layers. The domain size  $L_T[t=\tau_2(t_{w3})]$  becomes equal to the domain size  $L_T[t=\tau_1(t_{w3})]$  at  $T=T_{cl}$ .

In the low temperature phase below  $T_{cl}$ ,  $S_{ZFC}(t)$  shows a single peak at  $t=\tau(t_w)$ , where  $t_w$  is equal to either  $t_{w1}$  or  $t_{w3}$ . The characteristic time  $\tau(t_w)$  is linearly dependent on  $t_w$ :  $\tau(t_{w3})/\tau(t_{w1})=5.7$  at  $T=6$  K. This result indicates that there exist only domains with the size  $L_T[\tau(t_w)]$ . The domain sizes grow with increasing  $t_w$ . The domain size  $L_T[\tau(t_w)]$  may correspond to the size of correlated domains. The single peak of  $S_{ZFC}(t)$  vs  $t$  occurs at  $t=\tau(t_w)$  when the probing length  $L_T(t)$  is on the same order as the domain size  $R(t_w)$  after the aging protocol. The relaxation time  $\tau(t_w)$  tends to increase with decreasing  $T$  below  $T_{cl}$ .

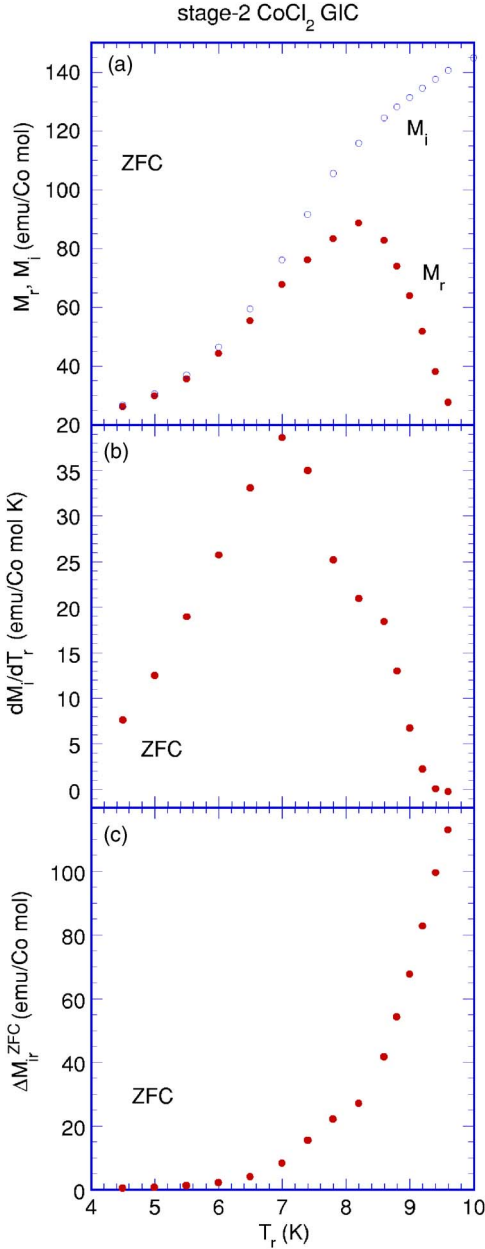


FIG. 14. (Color online) (a)  $T_r$  dependence of  $M_r$  and  $M_i$ .  $M_r$  and  $M_i$  are the value of  $M_{ZFC}$  at  $T=T_r$  and  $T_i (=3.0$  K), respectively, which are obtained in the measurement of  $M_{ZFC}$  with decreasing  $T$  from  $T_r$  to  $T_i$  [see Fig. 12(a)]. (b)  $T_r$  dependence of  $dM_i/dT_r$ . (c)  $T_r$  dependence of  $\Delta M_{ir}^{ZFC}$  ( $=M_i-M_r$ ).

### C. In-plane spin correlation length from the genuine TRM measurement

In the present work, we have not measured the  $t$  dependence of relaxation rate  $S_{TRM}(t)$  for the TRM magnetization. However,  $S_{TRM}(t)$  can be estimated as  $S_{TRM}(t) \approx -S_{ZFC}(t)$  using the fundamental link given by Eq. (3). From the results of Fig. 5(c) for  $S_{ZFC}(t)$  at  $T=8.0$  K, it is expected that  $S_{TRM}(t)$  at  $t_w=t_{w2}$  ( $=1.0 \times 10^4$  s) exhibits two negative local minima at  $t_{cr1}$  ( $=2.5 \times 10^3$  s) and  $t_{cr2}$  ( $=1.17 \times 10^4$  s). In the genuine TRM measurement (see Sec. III B), the system is aged at  $T=T_s$  for  $t_s=t_{w2}$  in the presence of  $H=H_c$  ( $=1$  Oe).

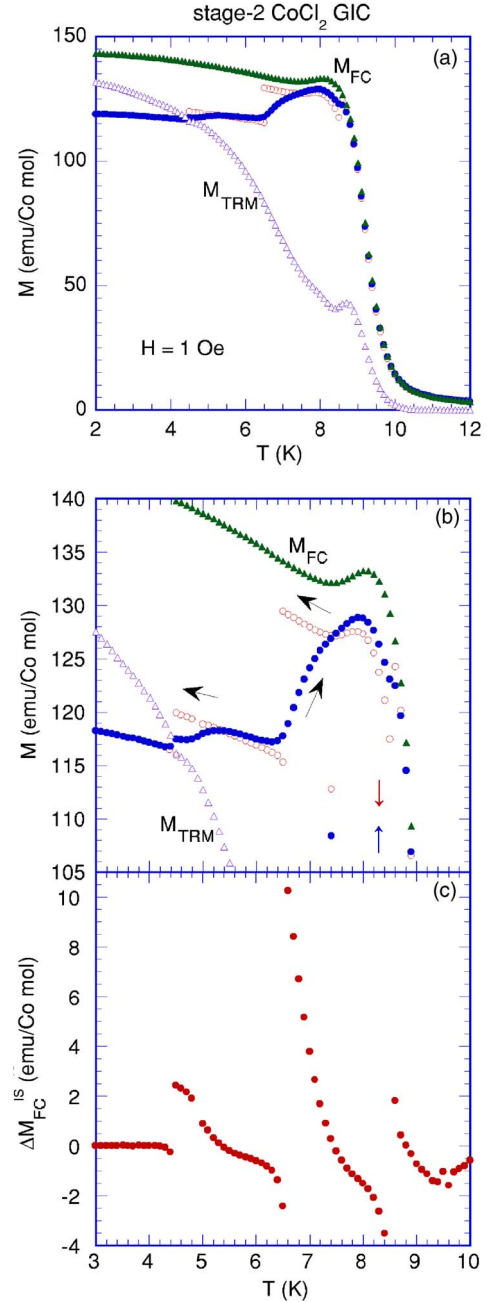


FIG. 15. (Color online) (a) and (b)  $T$  dependence of  $M_{FC}^{IS}(T_{\downarrow})$  ( $\circ$ ) and  $M_{FC}^{IS}(T_{\uparrow})$  ( $\bullet$ ) observed in the following FC aging protocol. The system was quenched from 50 to 12 K in the presence of  $H$  ( $=1$  Oe).  $M_{FC}^{IS}(T_{\downarrow})$  was measured with decreasing  $T$  from 12 to 1.9 K but with intermittent stops at  $T=8.5$ , 6.5, and 4.5 K for a wait time  $t_w=3.0 \times 10^4$  s. The field is cut off during each stop.  $M_{FC}^{IS}(T_{\uparrow})$  was measured at  $H=1$  Oe with increasing  $T$  after the above cooling process. The  $T$  dependence of  $M_{FC}^{ref}$  ( $\blacktriangle$ ) and  $M_{TRM}^{ref}$  ( $\triangle$ ) are also shown as reference curves. These are measured after the FC aging protocol without intermittent stop (reference curves). (c)  $T$  dependence of the difference  $\Delta M_{FC}^{IS} [=M_{FC}^{IS}(T_{\downarrow})-M_{FC}^{IS}(T_{\uparrow})]$ .

The above prediction for  $S_{TRM}(t)$  vs  $t$  with  $t_w=t_{w2}$  may suggest that two types of domains coexist, single island (domain) and correlated domains formed of small islands through interisland interactions. Since  $t_{cr2}$  is on the same



order as  $t_s$  ( $=1.0 \times 10^4$  s), the size of correlated domains is considered to reach the in-plane spin correlation length  $\xi_a(T_s)$  in thermal equilibrium. The correlated domains are frozen in when the FC cooling is resumed. These frozen states are reactivated when the system is reheated at  $T_s$ . The magnetization  $\Delta M_{\text{TRM}}(T=T_s; T_s, t_s)$  is approximated by  $g_a \mu_B S [\xi_a(T_s)/a]^2$ , where  $g_a$  ( $=6.4$ ) is the Landé  $g$ -factor of  $\text{Co}^{2+}$  spin along the  $a$  axis in the  $c$  plane,  $S$  ( $=1/2$ ) is a fictitious spin, and  $a$  is the in-plane lattice constant.<sup>1</sup> As shown in Fig. 4,  $(\Delta M_{\text{TRM}})_{\text{max}}$  increases with decreasing  $T_s$  from  $T_{cu}$  to  $T_{cl}$ . Correspondingly  $\xi_a(T_s)$  increases with increasing  $T_s$  and tends to diverge at  $T=T_{cl}$ .

#### D. Overlap length from the genuine TRM measurement

Here we discuss the effect of the overlap length on the genuine TRM magnetization (Sec. III B). The ordered domains generated at  $T=T_s$  are frozen in and survive the spin reconfiguration occurring at lower temperature on shorter length scales. The rejuvenation of the system occurs as the temperature is decreased away from  $T_s$ . Nevertheless, the spin configuration imprinted at  $T_s$  is recovered on reheating. In this sense, the system sustains a memory of an equilibrium state reached after a stop-wait process at  $T_s$ . The influence of the spin configuration imprinted at a stop-wait protocol is limited to a restricted temperature range around  $T_s$  on reheating. The width of this region may be assigned to the existence of an overlap between the spin configuration attained at  $T_s$  and the corresponding state at a very neighboring temperature ( $T_s + \Delta T$ ).

Here we introduce a concept of the overlap which is encountered in the SG system.<sup>13–15</sup> The SG equilibrium configurations at different temperatures at  $T$  and  $T + \Delta T$  are strongly correlated only up to the overlap length  $L_{\Delta T}$ , beyond which these correlations decay to zero. From the droplet theory, the overlap length  $L_{\Delta T}$  is proportional to  $1/|\Delta T|$ .<sup>25</sup> The width  $\Delta T$  is determined from the condition that  $R_{T_s}(t_s) = L_{\Delta T}$ .

In our system, the spin configuration imprinted during the stop-wait protocol at  $T=T_s$  for  $t=t_s$  is unaffected by a small temperature shift such that the overlap length  $L_{\Delta T}$  is larger

than the average domain sizes. There is a sufficient overlap between the equilibrium spin configurations at the two temperatures  $T_s$  and  $T_s + \Delta T$ . The situation is different when the temperature shift becomes large. The overlap length becomes shorter than the original domain sizes. A smaller overlap between spin configurations promotes the formation of broken domains. When the temperature shift is sufficiently large, the overlap length is much shorter than the original domain sizes, leading to the rejuvenation of the system.<sup>25–28</sup> The asymmetric form of  $\Delta M_{\text{TRM}}(T; T_s, t_s)$  around  $T=T_s$  ( $=7.6$  K) between  $T_{cl}$  and  $T_{cu}$  indicates that the spin configuration under the positive  $T$ -shift is different from that under the negative  $T$ -shift. We note that the appearance of the asymmetric form at  $T_s$  ( $=7.6$  K) is closely related to the diverging nature of the domain size  $L_T[\tau_2(t_{w3})]$  of correlated domains at  $T=7.5$  K [see Fig. 6(a)].

#### V. CONCLUSION

We have studied the aging dynamics of stage-2  $\text{CoCl}_2$  GIC between two magnetic phase transitions at  $T_{cl}$  ( $=7.0$  K) and  $T_{cu}$  ( $=8.9$  K). The observed aging phenomena are well explained within the framework of the droplet model for SG systems. The intermediate state between  $T_{cl}$  and  $T_{cu}$  has characteristic of both ordered and disordered states. A genuine TRM measurement indicates that the memory of the specific spin configurations imprinted at temperatures between  $T_{cl}$  and  $T_{cu}$  during the FC aging protocol can be recalled when the system is reheated at a constant heating rate. The ZFC and TRM magnetizations are examined in a series of heating and reheating processes. The magnetization shows both characteristic memory and rejuvenation effects. The time ( $t$ ) dependence of the relaxation rate  $S_{\text{ZFC}}(t)$  after the ZFC aging protocol with a wait time  $t_{w3}$  ( $=3.0 \times 10^4$  s) exhibits two peaks at characteristic times  $\tau_1(t_{w3})$  and  $\tau_2(t_{w3})$  at temperatures between  $T_{cl}$  and  $T_{cu}$ . These results suggest that two types of ordered domains coexist in the intermediate state. The intermediate state is a SG phase extending over ferromagnetic islands.

#### ACKNOWLEDGMENT

The authors would like to thank H. Suematsu for providing them with a single crystal of kish graphite.

\*Electronic address: suzuki@binghamton.edu

†Electronic address: itsuko@binghamton.edu

<sup>1</sup>T. Enoki, M. Suzuki, and M. Endo, *Graphite Intercalation Compounds and Applications* (Oxford University Press, Oxford, 2003), Chap. 7, p. 236. See also references therein.

<sup>2</sup>Y. Murakami, M. Matsuura, M. Suzuki, and H. Ikeda, *J. Magn. Mater.* **31-34**, 1171 (1983).

<sup>3</sup>M. Matsuura, Y. Endoh, T. Kataoka, and Y. Murakami, *J. Phys. Soc. Jpn.* **56**, 2233 (1987).

<sup>4</sup>D. G. Wiesler, M. Suzuki, and H. Zabel, *Phys. Rev. B* **36**, 7051 (1987).

<sup>5</sup>M. Matsuura, N. Tanaka, Y. Karaki, and Y. Murakami, *Jpn. J. Appl. Phys., Suppl.* **26-3-1**, 797 (1987).

<sup>6</sup>Y. Murakami and M. Matsuura, *J. Phys. Soc. Jpn.* **57**, 1056 (1988).

<sup>7</sup>M. Matsuura and M. Hagiwara, *J. Phys. Soc. Jpn.* **59**, 3819 (1990).

<sup>8</sup>M. Matsuura, Y. Murakami, and M. Hagiwara, *Physica A* **191**, 316 (1992).

<sup>9</sup>K. Miyoshi, M. Hagiwara, and M. Matsuura, *J. Phys. Soc. Jpn.* **65**, 3306 (1996).

<sup>10</sup>M. Suzuki and I. S. Suzuki, *Phys. Rev. B* **58**, 840 (1998).

<sup>11</sup>M. Suzuki, I. S. Suzuki, and T.-Y. Huang, *J. Phys.: Condens. Matter* **14**, 5583 (2002).

<sup>12</sup>Y. Sun, M. B. Salamon, K. Garnier, and R. S. Averback, *Phys. Rev. Lett.* **91**, 167206 (2003).

- <sup>13</sup>D. S. Fisher and D. A. Huse, Phys. Rev. Lett. **56**, 1601 (1986).
- <sup>14</sup>A. J. Bray and M. A. Moore, Phys. Rev. Lett. **58**, 57 (1987).
- <sup>15</sup>D. S. Fisher and D. A. Huse, Phys. Rev. B **38**, 373 (1988); **38**, 386 (1988); **43**, 10728 (1991).
- <sup>16</sup>R. Mathieu, P. Jönsson, D. N. H. Nam, and P. Nordblad, Phys. Rev. B **63**, 092401 (2001).
- <sup>17</sup>R. Mathieu, P. E. Jönsson, P. Nordblad, H. A. Katori, and A. Ito, Phys. Rev. B **65**, 012411 (2001).
- <sup>18</sup>S. Sahoo, O. Petracic, W. Kleemann, P. Nordblad, S. Cardoso, and P. P. Freitas, Phys. Rev. B **67**, 214422 (2003).
- <sup>19</sup>S. Sahoo, O. Petracic, W. Kleemann, S. Stappert, G. Dumpich, P. Nordblad, S. Cardoso, and P. P. Freitas, Appl. Phys. Lett. **82**, 4116 (2003).
- <sup>20</sup>N. Bontemps and R. Orbach, Phys. Rev. B **37**, 4708 (1988).
- <sup>21</sup>N. Bontemps, in *Heidelberg Colloquium on Glassy Dynamics*, edited by J. L. van Hemmen and I. Morgenstern (Springer-Verlag, Berlin, 1986), p. 66.
- <sup>22</sup>I. S. Suzuki and M. Suzuki, cond-mat/0603725 (unpublished).
- <sup>23</sup>C. Djurberg, J. Mattsson, and P. Nordblad, Europhys. Lett. **29**, 163 (1995).
- <sup>24</sup>M. Sasaki, P. E. Jönsson, H. Takayama, and H. Mamiya, Phys. Rev. B **71**, 104405 (2005).
- <sup>25</sup>L. Lundgren, in *Relaxation in Complex Systems and Related Topics*, edited by I. A. Campbell and C. Giovannella (Plenum, New York, 1990) p. 3.
- <sup>26</sup>P. Granberg, L. Sandlund, P. Nordblad, P. Svedlindh, and L. Lundgren, Phys. Rev. B **38**, 7097 (1988).
- <sup>27</sup>P. E. Jönsson, H. Yoshino, and P. Nordblad, Phys. Rev. Lett. **89**, 097201 (2002).
- <sup>28</sup>M. Suzuki and I. S. Suzuki, Eur. Phys. J. B **41**, 457 (2004).